Adv. Composite Mater., Vol. 16, No. 3, pp. 207–221 (2007)

Also available online - www.brill.nl/acm

Modeling of the filling process during resin injection/compression molding

CHIH-YUAN CHANG *

Department of Mechanical and Automation Engineering, Kao Yuan University, Lu-Chu, Taiwan 82101, R.O.C.

Received 24 November 2005; accepted 2 November 2006

Abstract—The filling process of resin injection/compression molding (I/CM) can be divided into injection and compression phases. During the resin injection the mold is kept only partially closed and thus a gap is present between the reinforcements and the upper mold. The gap results in preferential flow path. After the gap is filled with the resin, the compression action initiates and forces the resin to penetrate into the fiber preform. In the present study, the resin flow in the gap is simplified by using the Stokes approximation, while Darcy's law is used to calculate the flow field in the fiber mats. Results show that most of the injected resins enter into the gap during the injection phase. The resin injection time is extremely short so the duration of the filling process is determined by the final closing action of the mold cavity. Compared with resin transfer molding (RTM), I/CM process can reduce the mold filling time or injection pressure significantly.

Keywords: Injection/compression molding; resin transfer molding; filling process.

NOMENCLATURE [UNIT]

h	gap size [m]
h_{f}	height of fibrous reinforcement [m]
K_z	z-directional permeability of the fibrous reinforcement [m^2]
P	pressure [Pa]
P_{comp}	compression pressure [Pa]
P_{inj}	injection pressure [Pa]
P_{mat}	pressure of flow front in the fibrous reinforcement [Pa]
Re	Reynolds number in the gap

Edited by the JSCM.

*E-mail: yuan@cc.kyu.edu.tw

$\mathrm{Re_K}$ Reynolds number in the fibrous reinforcement
u, v, w velocity components in x, y, z direction [m/s]
V_{n-1}, V_n velocity of the front in the $(n-1)$th and nth time step [m/s]
x, y, z coordinate components in the physical domain [m]
X_{n-1}, X_n position of the front in the $(n-1)$th and nth time step [m]
z_{front} z-directional flow front [m]
Δt time interval [s]

Greek symbols

ξ, η coordinate components in the computational domain
Φ shape function
Ω, Ψ control functions in the body-fitted method
μ resin viscosity [Pa s]
ρ resin density [kg/m^3]

1. INTRODUCTION

In the processes of resin transfer molding (RTM), preformed fiber mats are preplaced in the mold cavity and resin is then injected into a closed mold filled with dry fiber reinforcement. This procedure provides the advantages of low resin injection pressure, fast cyclic periods and the ability to mold parts with highly complex shapes. However, one of the filling problems with RTM is the relatively high fiber volume content or large dimension of product. For these cases, it would take a long time to fill the mold cavity.

Resin injection/compression molding (I/CM) is a new variant of RTM process to enhance the fiber volume fraction and reduce the mold filling time. It incorporates the method of compression into the RTM. The combined injection and compression is performed in two steps as illustrated in Fig. 1. When the preform is placed in the mold cavity, the cavity remains partially closed. As a result, a gap is formed between the fibrous reinforcements and the mold. Resin can quickly fill up the gap during injection. Once the necessary amount of resin is injected, the mold platens are brought together, driving the resin through the preform and compacting the laminate to the final cavity thickness.

Brockmann and Michaeli [1] reported that the I/CM process showed a strong reduction of pressure compared to conventional injection molding. With same stress times it was possible to improve the parts quality using injection compression molding. Han *et al.* [2] proposed a numerical code that can be used to simulate the flow and heat transfer in injection/compression liquid composite molding (LCM). They reported that injection/compression LCM process could lead to more regular filling pattern and reduce the molding pressure significantly. Wirth and Gauvin [3] performed the experiments of compression resin transfer molding (CRTM). An

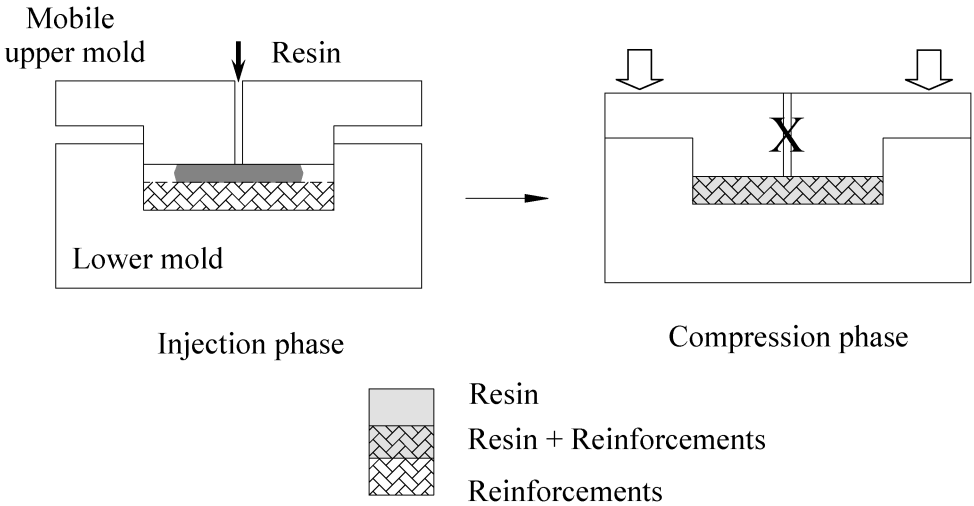

Figure 1. Schematic diagrams for the process of I/CM.

open gap was present on the top of the preform in the experiment. They reported that the resin injection time was extremely short and most filling and wetting time was elevated to the final closing of the cavity. Chang *et al.* [4] conducted the flow visualization experiment of compression transfer molding. They reported that the gap resulted in a preferential flow. Thus most resins entered into the gap and merely few resins penetrated through the fibrous reinforcements during injection. Chang [5] reported that using small gap size and high compression speed could achieve the minimum mold filling time for the simultaneous injection/compression molding process. However, the improper process parameters would cause the incomplete filling or reversed flow at the gate. Pham and Trochu [6] developed a two-dimensional finite element model for the CRTM process. The model allowed the study of the effect of compression on the filling of a composite part for different compression speeds and injection pressures. Kang and Lee [7] also proposed a numerical code to predict the resin flow, temperature, pressure and degree of cure distribution during resin transfer/compression molding (RT/CM). The compression force required for squeezing the impregnated preform can be calculated. Bickerton and Abdullah [8] utilized analytical solutions of simple flow geometries to explore the potential benefits of I/CM relative to RTM. Their model, based on elastic preform deformation, was used to explore the effect of process design parameters on resulting filling times, and clamping force requirements. Shojaei [9] developed a full three-dimensional numerical model by using control volume/finite element method for the resin I/CM process. The computer code could be conducted for the preform containing two and three layers of different reinforcements in various stacking sequences. Riche *et al.* [10] presented a methodology to study the effects of taking into account the resin transfer molding and compression (RTCM) process at early design stages. The model provided a clear description of how maximum

mold pressure, injection times and final structures properties are trade-off. Chang *et al.* [11] investigated the effects of process variables, including injection pressure, mold opening distance, resin temperature, compression pressure, pre-heated mold temperature and cure temperature, on the quality of CRTM products by using applying Taguchi's method.

For the aforementioned numerical works, the gap and the fibrous reinforcement are generally considered as a bulk porous medium. Resin flows through the fiber reinforcement in the planar direction. Thus a two-dimensional Darcy law is applicable during the filling process. The flows in the gap and in fiber mats are treated separately in the present study. During injection resin can quickly fill out the gap in the planar direction and a simplified penetrating velocity is proposed to understand the resin penetration into fiber mats. After that, the mold is closed and the resin is compressed and forced to penetrate the fibrous reinforcements in the thickness direction. In the present study, a numerical technique, body-fitted finite element method (FEM), is used to generate grids inside the physical domain and to calculate the flow behavior and other relative properties in the I/CM mold filling process. Simulations are also applied in RTM for comparison purposes.

2. THEORY

The I/CM mold filling process can be divided into injection and compression phases. Before the injection phase, a small gap is created between the reinforcements and the upper mold by pre-pressing fiber mats with the mobile mold. The gap results in preferential flow path because the flow resistance offered by the gap is much less than that offered by the fibrous preform. In order to clearly describe the flow phenomena, the x–y plane is set along the interface between the gap and the fibrous reinforcements and the z axis is upward. For the fluid flow in the small channel, several assumptions are made as follows.

1. The resin is a Newtonian fluid.
2. The filling process is quasi-steady state.
3. The inertial force is negligible compared to the viscous force due to Reynolds number less than unity.
4. The viscous shear term in z direction is larger than other directions according to the order of magnitude analysis.

Under the above assumptions, the continuity equation is

$$\frac{\partial u}{\partial x} + \frac{\partial v}{\partial y} + \frac{\partial w}{\partial z} = 0. \tag{1}$$

A simplified linear z-directional flow velocity in the gap is assumed and it satisfies the non-slip boundary condition at the upper mold and the penetrability along the interface between the gap and the fibrous reinforcements. We postulate that it may

be written as a product.

$$w(x, y, z) = w_0(x, y)\left(1 - \frac{z}{h}\right), \tag{2}$$

where w_0 denotes the penetrating velocity along the interface between the gap and the fibrous reinforcements and h is the height of the gap. The penetrating velocity can be governed by Darcy's law as follows.

$$w_0(x, y) = -\frac{K_z}{\mu}\left(\frac{\partial P}{\partial z}\right)_{z=0^-} \approx -\frac{K_z}{\mu}\left(\frac{P - P_{\text{mat}}}{z}\right), \tag{3}$$

where P_{mat} is the pressure of the flow front in the fibrous reinforcements. Here, the gauge pressure is adopted so P_{mat} is null; μ is resin viscosity and K_z is the z-directional permeability of the fiber mats. The physical meaning of permeability is the characteristic pore area in the fibrous preform. Since the flow area offered by the gap is much greater than that offered by the fibrous preform, the assumption of simplified penetrating velocity along the interface between the gap and the fibrous reinforcements is reasonable. Equation (2) is therefore generally valid.

The momentum equations for the resin flow in the gap are written as

$$\frac{\partial P}{\partial x} = \frac{\partial}{\partial z}\left(\mu\frac{\partial u}{\partial z}\right), \tag{4a}$$

$$\frac{\partial P}{\partial y} = \frac{\partial}{\partial z}\left(\mu\frac{\partial v}{\partial z}\right), \tag{4b}$$

$$\frac{\partial P}{\partial z} = \frac{\partial}{\partial z}\left(\mu\frac{\partial w}{\partial z}\right). \tag{4c}$$

Substituting equation (2) into (4c), the pressure gradient in the z direction is null. Therefore, the pressure equation can be obtained by differentiating equation (4a) with respect to x, differentiating equation (4b) with respect to y and adding the results.

$$\frac{\partial^2 P}{\partial x^2} + \frac{\partial^2 P}{\partial y^2} = 0. \tag{5}$$

Solving equations (1) and (5) and applying boundary conditions, the velocity field and pressure distribution in the gap can be calculated numerically. The physical domain and corresponding boundary conditions applicable to equation (5) are shown in Fig. 2.

For an infinitesimal time interval of the injection phase, the flow-induced penetration depth in the fibrous reinforcements can be obtained by substituting the velocity definition $w_0 = \phi(\mathrm{d}z/\mathrm{d}t)$ into equation (3); ϕ denotes the porosity of the fibrous reinforcements. The definition of the porosity in a porous media is

$$\phi = \frac{\text{pore volume}}{\text{total volume of porous media}} = \frac{\text{pore volume}}{\text{pore volume} + \text{fiber filament volume}}. \tag{6}$$

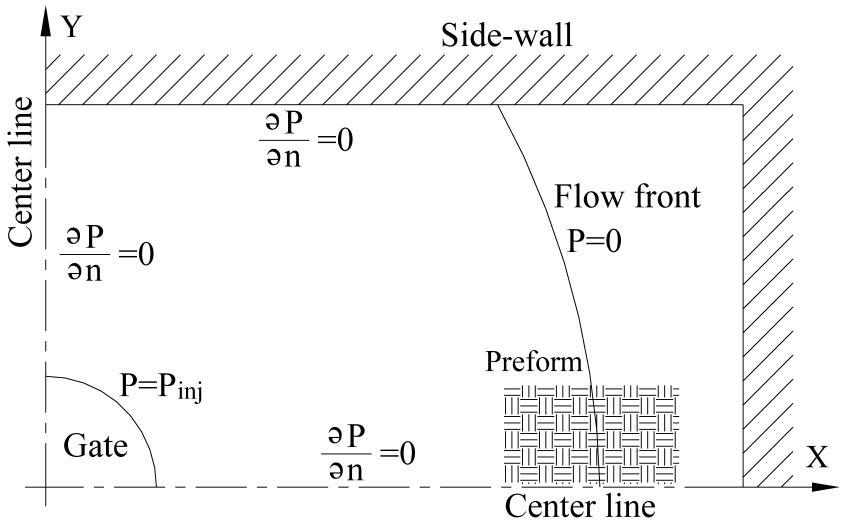

Figure 2. Boundary conditions.

Thus, we can sum up all the small time intervals and obtain the penetration depth at the given time.

$$z(x, y) = \sum_{i=1}^{n} \sqrt{\frac{2K_z}{\mu\phi}(P_i(x, y) - P_{\text{mat}})\Delta t_i} \tag{7}$$

where Δt is the time interval.

After the gap is fully filled with resin, the inlet gate is closed. The compression initiates and drives the resin through the preform. Since the fibrous preform is pre-pressed, the preform is assumed to undergo no further deformation during the mold filling. The penetrating process is assumed to be one-dimensional, since the mold thickness is much smaller than that in the plane direction. Thus, combination of continuity equation and Darcy's law gives us a governing equation that may be written as

$$\frac{\mathrm{d}}{\mathrm{d}z}\left(-\frac{K_z}{\mu}\frac{\mathrm{d}P}{\mathrm{d}z}\right) = 0. \tag{8}$$

The boundary conditions are

$$P(x, y, 0) = P_{\text{comp}} \text{ along the interface between gap and fiber mats,} \tag{9a}$$

$$P(x, y, z_{\text{front}}) = P_{\text{mat}} \text{ along the flow front within the fiber mats,} \tag{9b}$$

where P_{comp} is the compression pressure. Boundary condition (9a) interprets that the flow friction in the gap is negligible as compared with that in fibrous preform when the mobile upper mold forces the resin into the preform. Solving equation (8)

with boundary conditions (9), the pressure distribution can be obtained as follows.

$$P = P_{\text{comp}}\left(\frac{P_{\text{mat}}}{P_{\text{comp}}}\frac{z}{z_{\text{front}}} - \frac{z}{z_{\text{front}}} + 1\right). \tag{10}$$

3. NUMERICAL PROCEDURE

One of the difficulties of simulating the I/CM injection phase is the numerical treatment of the moving, irregular front surface of the resin. The body-fitted FEM (the combination of body-fitted grid generation with the finite element method) provides numerous advantages such as uniformly spaced grids, easily application of surface boundary conditions and modular technique, etc. It is well suited to solve the free moving boundary problem.

3.1. Galerkin's method

In the present FEM model, the method of weight residual adopts Galerkin's method. The Galerkin residual equation for governing equation (5) can be derived from

$$\int_A \int \left(\frac{\partial^2 P}{\partial x^2} + \frac{\partial^2 P}{\partial y^2}\right)\Phi_j \, \mathrm{d}x \, \mathrm{d}y = 0, \quad j = 1, 2, \ldots, 6, \tag{11}$$

where Φ_j is the shape function or trial function [12]. The element type applied in the present simulation is a 2-D, 6-nodal quadratic isoparametrical triangular element. The corresponding shape functions are

$$\begin{aligned}
\Phi_1(\xi, \eta) &= (1 - (\xi + \eta))(1 - 2(\xi + \eta)),\\
\Phi_2(\xi, \eta) &= \xi(2\xi - 1),\\
\Phi_3(\xi, \eta) &= \eta(2\eta - 1),\\
\Phi_4(\xi, \eta) &= 4\xi(1 - (\xi + \eta)),\\
\Phi_5(\xi, \eta) &= 4\xi\eta,\\
\Phi_6(\xi, \eta) &= 4\eta(1 - (\xi + \eta)),
\end{aligned} \tag{12}$$

where ξ and η are the local coordinates for each element. Integrating equation (11) by parts once and applying boundary conditions into the equation, the pressure distribution can be calculated numerically.

3.2. Nodal coordinates

The nodal coordinates of the present FEM scheme are generated by the body-fitted method. A set of elliptic partial differential equations is used as follows [13]:

$$\xi_{xx} + \xi_{yy} = \Omega(\xi, \eta)(\xi_x^2 + \xi_y^2), \tag{13a}$$

$$\eta_{xx} + \eta_{yy} = \Psi(\xi, \eta)(\eta_x^2 + \eta_y^2), \tag{13b}$$

where Ω and Ψ are the control functions. Interchanging the dependent variables (ξ, η) with the independent variables (x, y) in the above equations yields

$$a(x_{\xi\xi} + \Omega x_\xi) - 2bx_{\xi\eta} + c(x_{\eta\eta} + \Psi x_\eta) = 0, \tag{14a}$$

$$a(y_{\xi\xi} + \Omega y_\xi) - 2by_{\xi\eta} + c(y_{\eta\eta} + \Psi y_\eta) = 0, \tag{14b}$$

where $a = x_\eta^2 + y_\eta^2$, $b = x_\xi x_\eta + y_\xi y_\eta$ and $c = x_\xi^2 + y_\xi^2$. ξ and η are taken as coordinates in the computational domain. The control functions, based on the assumptions that the curvature along the geometric boundaries is locally zero and the grid lines are orthogonal to each other in the vicinity of geometric boundaries, are determined by

$$\Omega = -(x_{\xi\xi}x_\xi + y_{\xi\xi}y_\xi)/(x_\xi^2 + y_\xi^2), \tag{15a}$$

$$\Psi = -(x_{\eta\eta}x_\eta + y_{\eta\eta}y_\eta)/(x_\eta^2 + y_\eta^2) \tag{15b}$$

along the geometric boundaries. For the interior points, the control function is interpolated from that on the geometric boundaries.

The nodal coordinates are updated for each time step. For the purpose of saving computational space and time, the number of elements is proportional to the volume of filled liquid. An auto-transformation of numbering of nodes between the body-fitted finite difference method (FDM) and FEM is necessary in the pre-process of the FEM. Thus the body-fitted FEM is an auto-meshed scheme.

3.3. Numerical procedure

During the filling process, the resin progression can be calculated as follows.

1. Guess the position of the flow front in the nth time step by the formula of

$$X_n = X_{n-1} + V_{n-1} \times \Delta t.$$

   X_{n-1} and X_n denote the position of the front in the $(n-1)$th and nth time step, respectively. V_{n-1} is the velocity of the front in the $(n-1)$th time step.
2. Calculate the velocity and pressure fields.
3. Update the position of the flow front by the formula of $X_{n-1} + \Delta t \times (V_{n-1} + V_n)/2$, where V_n is the velocity of the front in the nth time step. Repeat steps 1–3 until the flow front converges to the correct position.
4. Calculate the flow-induced penetration depth in the fibrous reinforcements.
5. Repeat step 1 to step 5 until the injection finishes.
6. Calculate the penetration depth in the fibrous reinforcements in the compression phase.

4. EXPERIMENTAL

The random fiber mat (TGFM-300P/E) adopted in this study is made of 12 μm diameter strands chopped into 0.05 m length. The surface density of the fiber mat is

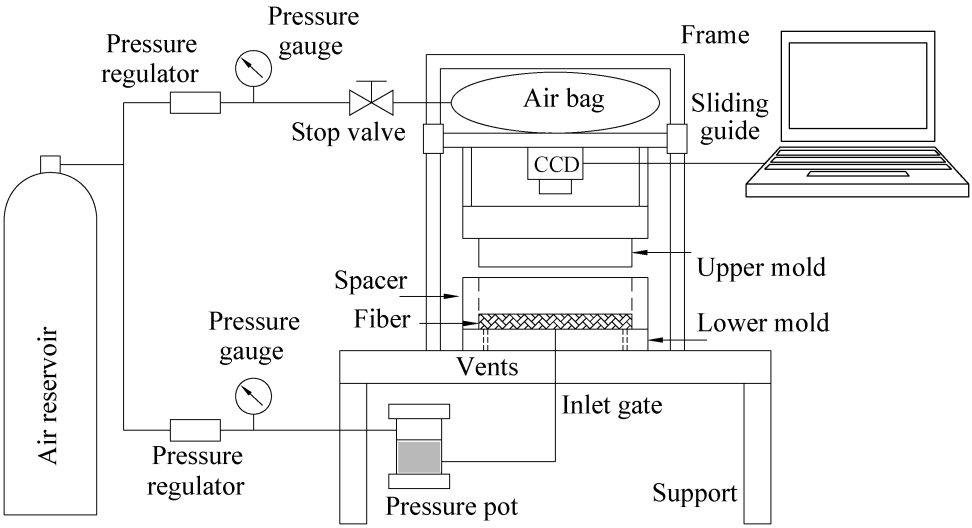

Figure 3. Experimental setup.

0.3 kg/m^2 and the density of the fiber filament is 2560 kg/m^3. The permeability is measured by flow visualization experiment [14]. The planar permeability is 1.03×10^{-10} m^2 and z-directional permeability is 5.8×10^{-11} m^2 at the porosity of 0.7, respectively. The density and viscosity of the engine oil (SAE 30) is 890 kg/m^3 and 0.29 Pa s in room temperature.

Figure 3 is a diagram of the experimental setup used to conduct the flow visualization experiments. The air-bag assisted compressible mold is designed to fit the requirement for the I/CM process. The mold consists of moving upper mold, spacer and lower mold. The upper mold and spacer are made of transparent acrylic to observe the flow behavior. To reduce friction and avoid leakage on the side of the mold, the upper mold is carefully cut, and a thin layer of grease is distributed on the mold wall as a lubricant. The lower mold is made of steel S45C. An inlet gate is constructed by cutting a hole about 16 mm in diameter on the center of the lower mold. At the same time, a hole is punched near the inlet gate into the fiber mats preplaced in the cavity so that there would be no flow resistance at the entrance. Before running the experiment, the fibrous preform is pre-pressed to the desired porosity by moving the upper mold down in order to create a small gap between the mold and fiber mats.

Resin is injected into the mold by using a pressure pot connected to a compressed air source. The injection pressure could be changed by pressure regulator adjusting the pressure of the air reservoir. An air bag is set above the upper mold. After the desired amount of resin is injected into the mold cavity, the air bag starts to inflate and then the upper mold moves downward. The closing action of the mold cavity forces the resin in the gap to penetrate into the fiber preform. Finally, the residual resin is squeezed out of the cavity from the vents.

The advancing flow front is recorded on the videotape by the CCD camera. The camera fixed above the upper mold is used to take a picture of the flow front in the plane direction during the injection phase. The primary picture of the desired flow front position is transformed from the videotape by the multimedia packaged software and the Multi-video interface.

5. RESULTS AND DISCUSSION

During the filling process of the I/CM, the injection and compression condition can be either a constant velocity/flow rate or a constant pressure. Here, a constant applied pressure is taken as the injection and compression conditions.

Figure 4 shows the flow front of the resin at various times during the injection phase. As the mold is partially closed, a gap is formed between the fiber mats and mold. This gap results in a preferential flow. Figure 4(a) shows the flow front progression in the gap. The plot is a diagram of top view. Before the flow front contacts the side wall, the fluid expands radially in the gap. After the flow front contacts the side wall, the fluid is gradually transformed from a radial flow to a uniform flow since the fluid flow is restricted by the side walls. The experimental flow front is also denoted by a dashed line as shown in Fig. 4(a). Apparently the flow fronts obtained by the numerical prediction are close to the experimental data. While most resins enter into the gap in the injection phase, few resins can penetrate into the fibrous reinforcements as shown in Fig. 4(b). For the sake of clear explanation, the plot is a diagram of the side view along the plane of the x–z axis. Obviously, the high resistances of the fibrous reinforcements make it difficult for the resin to penetrate into the fiber mats. The results validate the previous assumption. The Reynolds number in the gap is defined as $\mathrm{Re} = \rho v h/\mu$. Calculation of the Re during the injection phase gives a value of $\mathrm{Re} \approx 10^{-1}$ at the injection pressure of 0.345 kPa. The flow is creeping motion due to low Re.

The velocity distribution at the time of 3.88 s, as shown in Fig. 5, illustrates the tendency of flow transformation from a radial flow to a uniform flow as mentioned above. It is found that the velocity decreases gradually from the inlet gate to the flow front. This is because that the friction between the fluid and the fibrous preform increases gradually as the contacting area increases.

After the injection ends, the mold is closed and then resin is forced to penetrate through fiber networks. Figure 6 shows the resin impregnation position at various times during the compression phase. In the plot, the scale ratio of x-axis to z-axis is 1 to 5. As a result of the high pressure gradient in the thickness direction, the resin flow is almost uniform in the compression phase even though there are few resins penetrating into the fibrous reinforcements in the injection phase. It is worth noting that the flow is much slower in the compression phase than that in the injection phase even if the compression pressure is twenty times the magnitude of the injection pressure in the case. The reason is that the low permeability of the fibrous reinforcements results in high flow resistance. This implies that the total

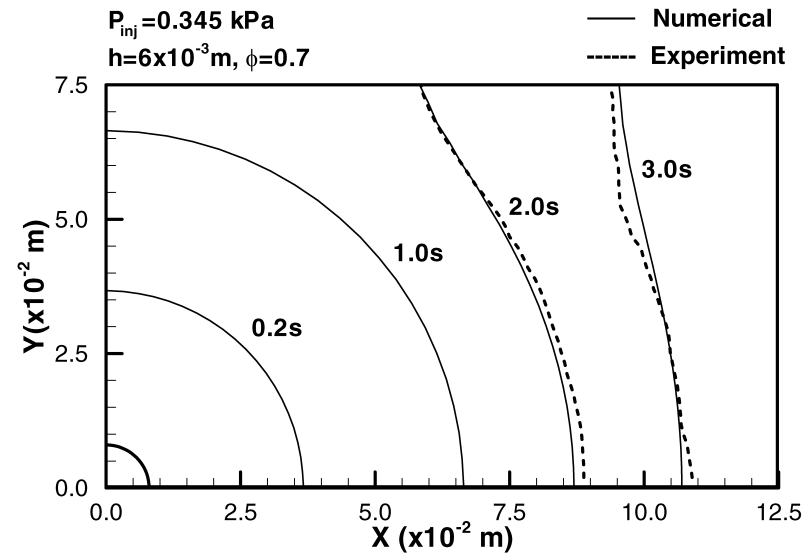

(a)

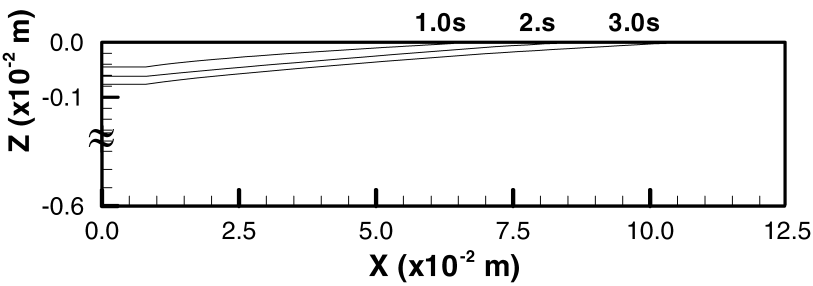

(b)

Figure 4. Flow front of the resin at various times during the injection stage. (a) Flow front in the gap. (b) Flow front in the fibrous reinforcements.

mold filling time mainly depends on the duration of the compression phase. That is to say, most filling time is determined by the final closing action of the mold cavity. The results imply that adopting the high compression pressure may be an effective method for reducing the I/CM filling time. For a porous medium, the Reynolds number is defined as $\mathrm{Re_K} = \rho v \mathrm{K}^{1/2}/\mu$. During the compression phase, the $\mathrm{Re_K}$ is about 10^{-2}–10^{-3}. Since $\mathrm{Re_K}$ is much less than 1, the viscous force is significant and Darcy's law is valid.

Figure 7 shows the simulated history of the clamping force. The force exerted on the mold platens due to fluid pressure is found by integrating across the wetted portion of the mold. Apparently, the clamping force is increasing gradually in the injection phase due to the fact that the wetted portion increases. After

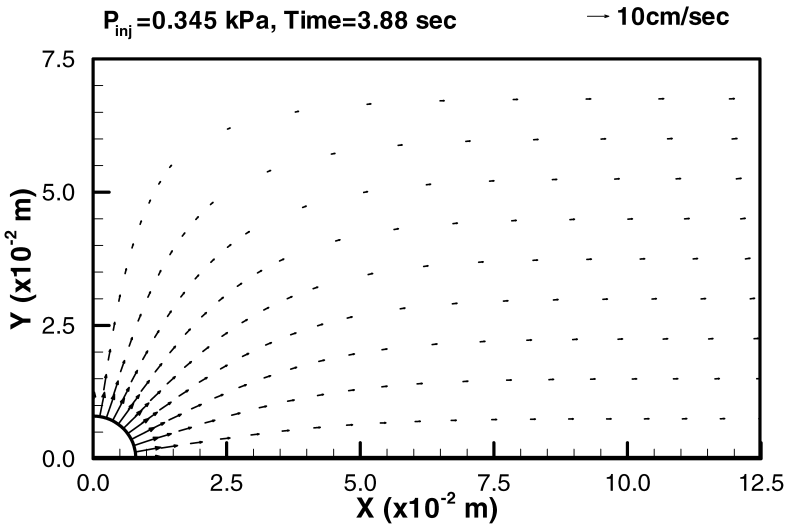

Figure 5. The velocity distribution at the time of 3.88 seconds in the injection phase.

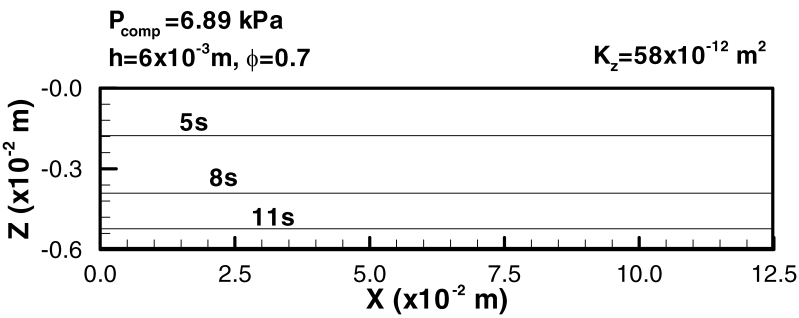

Figure 6. Resin impregnation position along the plane of x–z axis at various times during the compression phase.

the compression phase proceeds, the wetted portion increases no more and thus clamping force is constant.

A relationship between the total filling time and the applied pressure is shown in Fig. 8. The injection pressure is equal to the compression one in the I/CM processes. The RTM process can be regarded as a special I/CM case in which the mold opening gap is null. The resin injection time decreases with the large gap and applied pressure during injection since the high applied pressure can speed up the resin velocity and the large gap can reduce the flow resistance offered by the gap. However, the overlarge gap can cause too much injected resin. It takes much time to squeeze the residual resin out of the cavity during compression due to the high flow resistance of the fibrous reinforcements. Therefore, there is a maximum reduction of the mold filling time in the I/CM process with a small gap. Note that an incomplete filling process will occur for the case of using too small a gap since the volume of the resin in the gap is less than the pore volume of fiber mats. That is

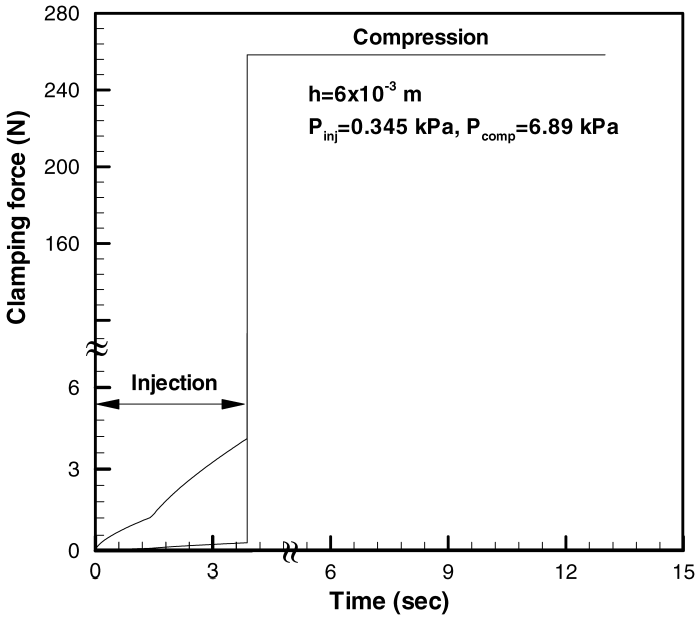

Figure 7. The simulated history of the clamping force.

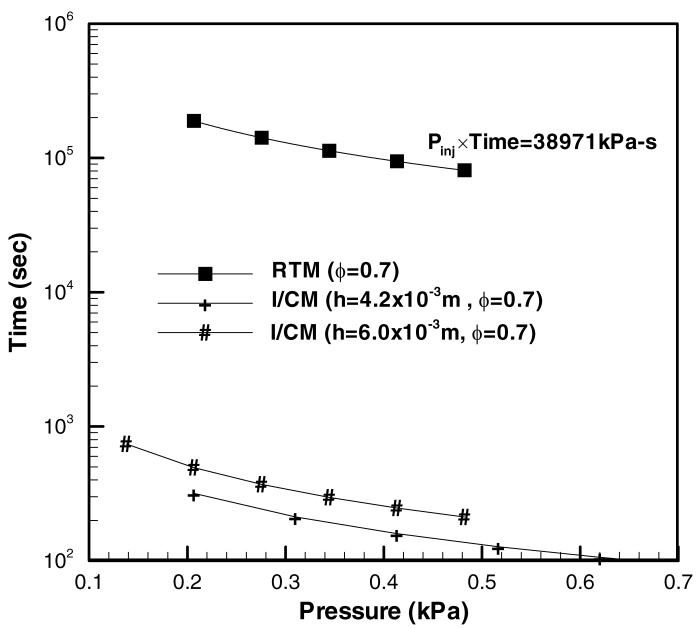

Figure 8. A relationship between the total filling time and the applied pressure.

to say, an admissible gap size can be expressed by

$$h \geqslant \phi h_{\mathrm{f}}, \tag{16}$$

where h_{f} is the height of the fibrous reinforcements. Moreover, the data concerning RTM can be exactly fitted by hyperbolic curves due to the similarities of the governing equation and boundary conditions [15]. Compared with RTM, the I/CM process can reduce significantly the mold filling time or injection pressure by extending RTM data in the pressure axis to the same filling time.

6. CONCLUSIONS

A numerical technique, body-fitted finite element method, is used to calculate the flow behavior and other relative properties in the I/CM mold filling process. In the present study, the fiber mats are pre-pressed and thus a gap is present on the top of the preform. Results show that most of the injected resins enter into the gap during injection. The fluid is gradually transformed from a radial flow to a uniform flow for the case of rectangular mold with center gate. The resin injection time is extremely short and most filling time is determined by the final closing action of the mold cavity. This infers that adopting a high compression pressure is an effective method for reducing the filling time. There is a maximum reduction of the mold filling time in the I/CM process with small gap. Note that there is a minimum admissible gap below which an incomplete filling process will occur. Compared with RTM, the I/CM process can reduce the mold filling time or injection pressure significantly.

REFERENCES

1. C. Brockmann and W. Michaeli, Injection compression molding – a low pressure process for manufacturing textile-covered mouldings, *ANTEC'97* **1**, 441–445 (1997).
2. K. Han, J. Ni, J. Toth, L. J. Lee and J. P. Greene, Analysis of an injection/compression liquid composite molding process, *Polym. Compos.* **19**, 487–496 (1998).
3. S. Wirth and R. Gauvin, Experimental analysis of mold filling in compression resin transfer molding, *J. Reinf. Plast. Compos.* **17**, 1414–1430 (1998).
4. C. Y. Chang, L. W. Hourng and C. S. Yu, Analysis of flow phenomena during the filling stage of CTM, *J. Reinf. Plast. Compos.* **23**, 1561–1570 (2004).
5. C. Y. Chang, Simulation of mold filling in simultaneous resin injection/compression molding, *J. Reinf. Plast. Compos.* **25**, 1255–1268 (2006).
6. X. T. Pham and F. Trochu, Simulation of compression resin transfer molding to manufacture thin composite shell, *Polym. Compos.* **20**, 436–459 (1999).
7. M. K. Kang and W. I. Lee, Analysis of resin transfer/compression molding process, *Polym. Compos.* **20**, 293–304 (1999).
8. S. Bickerton and M. Z. Abdullah, Modeling and evaluation of the filling stage of injection/compression moulding, *Compos. Sci. Technol.* **63**, 1359–1375 (2003).
9. A. Shojaei, A numerical study of filling process through multilayer preforms in resin injection/compression molding, *Compos. Sci. Technol.* **66**, 1546–1557 (2006).

10. R. L. Riche, A. Saouab and J. Br'eard, Coupled compression RTM and composite layup optimization, *Compos. Sci. Technol.* **63**, 2277–2287 (2003).
11. C. Y. Chang, L. W. Hourng and T. Y. Chou, Effect of process variables on the quality of compression resin transfer molding, *J. Reinf. Plast. Comp.* **25**, 1027–1037 (2006).
12. D. S. Burnett, *Finite Element Analysis*. Addison-Wesley Publishing Company, Singapore (1988).
13. P. D. Thomas and J. F. Middlecoff, Direct control of the grid point distribution in meshes generated by elliptic equation, *AIAA J.* **18**, 652–656 (1980).
14. C. J. Wu, Numerical simulation on the edge effect of resin transfer molding, PhD Diss., Mech. Eng. Dept., National Central University, Taiwan (1995).
15. C. Y. Chang and L. W. Hourng, Numerical simulation for the transverse impregnation in resin transfer molding, *J. Reinf. Plast. Comp.* **17**, 165–182 (1998).